J Geophys (1981) 50: 89–100

Journal of Geophysics

On Modelling the Lithosphere in Mantle Convection with Non-Linear Rheology

H. Schmeling and W.R. Jacoby*

Institut für Meteorologie und Geophysik, Johann Wolfgang Goethe-Universität, Feldbergstr. 47, D-6000 Frankfurt 1, Federal Republic of Germany

Abstract. Numerical convection experiments were carried out with the aim of simulating the lithosphere as a strong mechanical boundary layer participating in the circulation, and to study its dynamical role and the governing parameters. The rheological model parameters were successively refined, effective viscosity depending on (1) depth, (2) temperature and pressure, and (3) temperature, pressure, and stress. In all cases a high-viscosity plate rested on a low-viscosity asthenosphere; in the two latter cases it could in principle subduct, but did so only if zones of weakness were built into it. It was possible to model active or inactive plates (moving faster or slower than the asthenosphere below). Because of a lack of numerical resolution it was however, not possible to simulate a narrow sinking slab; rather a broad zone of cooled and highly viscous material developed, often limiting the rate of descent and leading to non-steady convection. The circulation, including subduction, was stabilized by introduction of stress-dependence of viscosity (non-linearity), dissipation, and adiabatic heating. The parameter chiefly responsible for deciding the (active or passive) role of the plate is its decoupling from its neighbours, achieved in the models by assuming weakness zones. Another important result seems to be that the assumption of plausible mantle rheologies and heat input leads to equally plausible effective viscosities, plate velocities, and to upper-mantle temperatures which are relatively low by current ideas, but conforming to earlier estimates based on convection theory. Viscosity distribution and flow pattern are also in reasonable agreement with more detailed boundary layer computations. The main obstacles to our modelling are the numerical limitations, forcing upon us such artificialities as two-dimensionality, rectangular model boxes, coarse grids, and generalized weakness zones.

Key words: Mantle convection – Finite-difference model – Rheology – Mantle temperatures – Lithosphere

Introduction

The aim of our numerical experiments of mantle convection has been to model the lithosphere and its role in the whole circulation. Most previous studies have stressed either the aspect of thermal convection *or* the mechanical aspect of plate sliding and sinking. The gap between the two approaches is chiefly the consequence of the deficiencies of the modelling procedures available. Nevertheless, we try with limited means to gain some understanding of earth dynamics.

A model of mantle convection should include the plates to be realistic. They provide reliably known kinematic boundary conditions (rigid rotations typically of about 10^{-16} rad/s relative to each other: Minster et al. 1974; Minster and Jordan 1978). The outline of the plates varies with time and their lateral boundaries migrate in any frame of reference. Furthermore, simple force estimates (Jacoby 1970; Richter and McKenzie 1978) and global force equilibrium models (Forsyth and Uyeda 1975; Solomon et al. 1975; Harper 1975; Chapple and Tullis 1977) demonstrate that the gravitational instability of the plates plays an important role in mantle dynamics.

Little is known about the flow at depth. For continuity some large scale circulation must occur. Concentration of flow is evident in the descending slabs above 700 km depth. Plumes or jets (Morgan 1971; Artyushkov 1968; McKenzie et al. 1980) and small-scale longitudinal rolls (Richter 1973a; Richter and Parsons 1975) shall be disregarded, also such processes as phase changes and chemical differentiation, possibly stabilizing or destabilizing the mantle (Schubert and Turcotte 1971; Richter 1973b; Gebrande 1975; Schubert et al. 1975; Artyushkov 1968).

We assume that the convection is driven by thermally generated density differences. This assumption is convenient as thermal convection has been well studied since Bénard (1900) and Rayleigh (1916); it is also plausible (Tozer 1967a, b), the overcritical Rayleigh number Ra/Ra_c being very large ($Ra = \frac{g\alpha \Delta T L^3}{\nu\kappa}$; α = thermal expansivity; ΔT = temperature drop from bottom to top; L = vertical extent; g = gravity; κ and ν = diffusivities of temperature and momentum (kinematic viscosity); Ra_c = critical Rayleigh number of order 10^3 for the mantle: Jeffreys 1926; Chandrasekhar 1953; 1961). Even in the simplest case of constant material properties in an infinite horizontal layer heated from below or within and with any conceivable boundary conditions, a Rayleigh number as large as $100 \cdot Ra_c$ implies vigorous convection in rather flat non-steady cells (Busse 1967; Roberts 1967; Krishnamurti 1970a, b; Busse and Whitehead 1971). An important feature of such high-Rayleigh-number convection is the development of pronounced thermal boundary layers which particularly concern us here.

* *Present address:* Institute of Geophysics and Planetary Physics University of California Los Angles, Los Angeles, CA 90024, USA

0340-062X/81/0050/0089/$02.40

The mantle is, however, more complicated than that. It is not homogeneous; its properties, particularly viscosity, are temperature and pressure dependent. Thermal boundary layers thus also become mechanical ones. Stratified models (including those with a rigid lithosphere) can concentrate the flow at shallow depth (Foster 1969; Takeuchi and Sakata 1970) with large aspect ratios (Gebrande 1975; Houston and DeBremaecker 1975; Richter and Daly 1978; Daly 1980), but they do not exclude convection cells of great depth extent (Davies 1977). A step forward in modelling is to include the lithospheric descent by simply assuming the desired geometrical structure of "rigid" slabs (Richter 1973a; Richter and McKenzie 1978) or high-viscosity regions (Kopitzke 1979) or lateral thermal boundary conditions (Rabinowicz et al. 1980); the flow is then highly organized by the assumed structure. In a more realistic model such a structure should develop by itself as a result of temperature (T), pressure (p), and stress (τ) dependence of rheology. The problem becomes complex and highly non-linear because flow and temperature interact with the mantle properties. Studies of *sub*-lithospheric convection with T, p dependent linear rheology (Torrance and Turcotte 1971; Turcotte et al. 1973; Rabinowicz et al. 1980) and with only τ or with T, p, τ dependent non-linear rheology (Parmentier et al. 1976; Rabinowicz et al. 1980) suggest that the interaction of the material properties with the flow is not too critical. However, inclusion of the lithosphere complicates matters. Houston and DeBremaecker (1975) and DeBremaecker (1977) used T, p or T, p, τ dependent rheologies, while Daly (1980) used T-dependent rheologies, to simulate the lithosphere, but it was either immobile, if too thick and/or too viscous, or it deformed non-rigidly, if too thin and/or too soft.

Approach to Convection with Lithosphere Participating

We have followed a strategy of proceeding from simple stratified models to similar ones with built-in weakness zones, then to models with T, p dependent linear rheologies, and finally to models with non-linear T, p, τ dependent rheologies. These, too, were modified locally by weakness zones necessary to mobilize the lithosphere (see also Kopitzke 1979). In addition, we tested the effects of adiabatic heating/cooling and of dissipation.

The physics of the problem is described by the conservation of mass, i.e., continuity (ρ=density; $\mathbf{v}=(v_1, v_2, v_3)$ =velocity; $\partial_i=\partial/\partial x_i$, x_i=coordinate, $i=1, 2, 3$):

$$\partial\rho/\partial t+\partial_i(\rho v_i)=0 \tag{1}$$

conservation of momentum - Navier-Stokes equation (D/Dt =material derivative with time t; p=pressure; σ_{ij}=deviatoric viscous stress tensor; $\mathbf{g}=(0, 0, g)$=gravity; $\hat{\mathbf{z}}$=unit vector in x_3 direction):

$$D(\rho v_i)/Dt=-\partial_i p+\partial_j\sigma_{ij}+\rho g\hat{\mathbf{z}} \tag{2}$$

and conservation of energy (T=temperature; c_p=isobaric heat capacity; k=thermal conductivity; $\mathscr{H}$=volumetric heating; α=thermal expansivity)

$$\rho c_p DT/Dt-\alpha TD\,p/Dt=\partial_i(k\partial_i T)+\sigma_{ij}\partial_j v_i+\mathscr{H} \tag{3}$$

as well as the constitutive equations to be discussed later.

To obtain the dynamic pressure P, we subtract from p the hydrostatic pressure $\rho g x_3$ (x_3 positive downward); we introduce the equation of state $\rho=\rho_0(1+p/K-\alpha(T-T_0))$ where K is incompressibility; the viscous stress tensor has the form

$$\sigma_{ij}=\eta((\partial_j v_i+\partial_i v_j)-\tfrac{2}{3}\delta_{ij}\partial_i v_i)+\tfrac{1}{3}\eta^*\delta_{ij}\partial_i v_i$$

with η=dynamic viscosity and η^*=volume viscosity, neglected; δ_{ij}=Kronecker delta. We non-dimensionalise the equations following Turcotte et al. (1973).

All mantle properties except viscosity were assumed constant; their values (including reference viscosity ν_0) are given in Table 1. Table 2 lists typical values of the other variables. With these values the non-dimensionalisation allows us to neglect all terms which contribute no more than a few percent. We are left with the following dimensionless equations, with $\theta=T/T_c$ dimensionless, T_c characteristic temperature:

$$\partial_i v_i=0 \tag{1a}$$

$$\partial_i P-\partial_j\sigma_{ij}-Ra_0\,\theta\cdot\hat{\mathbf{z}}=0 \tag{2a}$$

$$D\theta/Dt+Di\cdot\theta\cdot v_3=\nabla^2\theta+Di/Ra_0\cdot\sigma_{ij}\partial_j v_i+H. \tag{3a}$$

H is the dimensionless internal heating per volume. Dissipation $Di/Ra_0\cdot\sigma_{ij}\partial_j v_i$ and adiabatic heating $Di\cdot\theta\cdot v_3$ are in-

Table 1. Assumed mantle properties and other model parameters

Symbol	Value	Meaning
η	=variable	dynamic viscosity
ν_0	$=\eta_0/\rho_0=3\ 10^{18}$ m^2/s	kinematic reference viscosity
K	$=10^{13}$ Pa	incompressibility
α	$=3.7\ 10^{-5}$ K^{-1}	thermal expansivity
κ	$=1.01\ 10^{-6}$ m^2/s	thermal diffusivity
c_p	$=10^3$ J/kg · K	isobaric heat capacity
$\mathscr{H}$	$=6.65\ 10^{-8}$ W/m^3	volumetric heating rate
ρ_0	$=3.5\ 10^3$ kg/m^3	reference density
Constants appearing in rheological equations		
R	=8.31 J/K mol	gas constant
k	$=1.38\ 10^{-23}$ J/K	Boltzmann's constant
f (Eq. 4)	=147 (or 21)	factor for superplasticity (or Nabarro-Herring creep)
Parameters assumed for olivine		
n; A	=2; 4 10^{-3} or 3; 3 10^{-6}	Dorn's parameters
b	$=6.98\ 10^{-10}$ m	Burgers vector
D_{v_0}; D_{B_0}	$=10^{-1}$ m^2/s	diffusivities: lattice; grain boundary
E_v, E_B	$=(5.4; 3.6)\ 10^5$ J/mol	activation energies (as above)
V_v	$=1.1\ 10^{-5}$ m^3/mol	activation volume
$\Omega(O^{--})$	$=1.15\ 10^{-29}$ m^3	volume of diffusing species (O^{--})
μ	$=\mu_0\left(1+\frac{1}{\mu_0}\frac{\partial\mu}{\partial T}(T-T_0)+\frac{1}{\mu_0}\frac{\partial\mu}{\partial p}(p-p_0)\right)$	rigidity
μ_0	$=7.91\ 10^{10}$ Pa	rigidity at surface conditions
$\frac{1}{\mu_0}\frac{\partial\mu}{\partial T}$	$=-1.4\cdot10^{-4}$ K^{-1}	relative temperature derivative of rigidity
$\frac{1}{\mu_0}\frac{\partial\mu}{\partial p}$	$=2.2\ 10^{-11}$ Pa^{-1}	relative pressure derivative
d	$=10^{-3}$ to 10^{-1} m	average grain size
δ	$=1.4\cdot10^{-9}$ m	grain boundary width

Table 2. Typical values of the variables in mantle convection

Variable	Symbol	Assumed	
		Dimensional	Non-dimensional value
Depth of convection	L	700 km	1
Aspect ratio (assumed)	λ	3 to 4	3 to 4
Time	t	> 1 Ma	$>6\ 10^{-5}$
Velocity	v	$\leqq$ 10 cm/a	$\leqq$ 2 000
Hydrostatic pressure	p_h	$\leqq 2.3\ 10^{10}$ Pa	$\leqq 3\ 10^6$
Dynamic pressure	P	$\leqq 10^8$ Pa	$\leqq 10^5$
Shear stress	τ	$\leqq 10^8$ Pa	$\leqq 10^5$
Temperature	T	$\leqq$ 2 000 K	$\leqq 2$
Characteristic temperature	T_c	1 000 K	1
Gravity	g	10 m/s^2	$3.4\ 10^{30}$
(with constants of Table 1:)			
Rayleigh number (scaling)	Ra_0	$=\frac{\alpha g T_c L^3}{\kappa_0 \nu_0}$	$=123\,653$
Dissipation number	Di	$=\frac{\alpha g L}{c_p}$	$=0.199$
Prandtl number	Pr	$=\frac{\nu_0}{\kappa_0}$	$=10^{24}$

cluded in some, but not all, models in order to investigate their influence. $Ra_0 = \frac{g \cdot \alpha \cdot T_c \cdot L^3}{\nu_0 \kappa}$ is the non-dimensionalisation Rayleigh number. To compute the effective Rayleigh number of a particular model, we have used the averaging procedure proposed by Parmentier et al. (1976). The Boussinesq approximation is implied, involving incompressibility in the above equations, but we deviate from this in the adiabatic heating term.

We assume two-dimensionality and introduce the stream function $\psi(x, z)$ with $\mathbf{v} = (\partial\psi/\partial z, -\partial\psi/\partial x)$ satisfying Eq. (1a) and obtain the final form of the Navier-Stokes equation ($\nu = \eta/(\rho_0 \nu_0)$, dimensionless kinematic viscosity)

$$4\frac{\partial^2}{\partial x \partial z}\left(\nu \frac{\partial^2 \psi}{\partial x \partial z}\right) + \left(\frac{\partial^2}{\partial z^2} - \frac{\partial^2}{\partial x^2}\right)\left(\nu \cdot \left(\frac{\partial^2}{\partial z^2} - \frac{\partial^2}{\partial x^2}\right)\psi\right) = Ra_0 \frac{\partial \theta}{\partial x} \qquad (2b)$$

and the energy equation:

$$\frac{\partial \theta}{\partial t} + \frac{\partial \psi}{\partial z}\frac{\partial \theta}{\partial x} - \frac{\partial \psi}{\partial x}\frac{\partial \theta}{\partial z} - Di\ \theta \frac{\partial \psi}{\partial x} = \frac{\partial^2 \theta}{\partial x^2} + \frac{\partial^2 \theta}{\partial z^2} + \frac{Di}{Ra_0} \cdot \nu \cdot \left(4\left(\frac{\partial^2 \psi}{\partial x \partial z}\right)^2 + \left(\frac{\partial^2 \psi}{\partial x^2} - \frac{\partial^2 \psi}{\partial z^2}\right)^2\right) + H. \qquad (3b)$$

These equations were solved numerically on a 21×21 mesh in square model boxes 700 km deep and $\lambda \cdot 700$ km wide (λ = aspect ratio, variable). Earth curvature was neglected. The boundary conditions were: *sides* closed, free slip, no heat transfer (implying symmetry about the lateral boundaries and periodic repetition of the cells); *top* closed, free slip, temperature 0° C; *bottom* closed, no slip or free slip, heat flow into the box 16 mW/m^2. Internal heat generation was assumed $6.65\ 10^{-8}$ W/m^3; the total heat input thus provides for a steady-state average loss of 60 mW/m^2 (Chapman and Pollack 1975) through the surface. In most cases of temeperature dependent rheology there was little difference between the no-slip and the free-slip condition at the bottom because a hot fluid lower boundary layer developed. The artificial assumptions, such as two-dimensionality, closed square model boxes, coarse grid, were dictated by our computational means and economy. They do present a serious limitation, but they may still help us in uncovering principal systematics in the role of the lithosphere. Even though details may not be quantitatively exact, we believe that our major conclusions are correct. We shall discuss this where appropriate.

Equation (2b) was approximated by a finite difference scheme similar to that of Andrews (1972) and was solved with the Gauss algorithm of elimination (Zienkewicz 1971, p. 462; see also Schmeling 1979; 1980). Equation (3) was solved with the alternating direct implicit (ADI) scheme used by Houston and DeBremaecker (1974). To ensure numerical stability, the time step occasionally had to be adjusted in model runs with T, p, τ dependent rheologies, as regions of low effective viscosity developed. This was done by hand with the aid of an interactive program (Schmeling 1979; 1980), facilitating the compromise between model progress and stability. It also lends credibility to the results.

Accuracy, stability, and convergence of the computations were tested against simple models (homogeneous material, free-slip boundaries, fixed temperature drop ΔT) with known analytical solutions. The results were unaffected by the initial conditions, and within limits, by the time step and grid spacing. The theoretical stability fields, as a function of aspect ratio, were exactly reproduced. Comparisons were run with published, more complex models (Houston and DeBremaecker 1975) and their amplitudes were reproduced to within 10–20%. Flow patterns were reproduced better. Only in cases of extreme rheology do we expect errors of flow amplitude and temperature greater than 20%.

Discussing our results, we shall focus on the comparison with aspects of mantle convection on which we have some information. Such aspects are surface velocities, rigid plate structure, and heat flow. Aspects of special interest include the stability or instability of cellular flow and the mantle temperatures. Observables such as topography, gravity (McKenzie 1977) and lithospheric stress (Richardson et al. 1979) will not be discussed here.

Results

The initial models investigated have a layered viscosity $\eta(z)$. In the first example (Fig. 1) the viscosity-depth distribution is that of McConnell (1968; model 62-12) who based his analysis on data from glacio-isostatic rebound of Precambrian shields. This viscosity is probably appropriate to such regions. It is characterized by a rather thick (120 km) high-viscosity lithosphere overlying an asthenosphere of 10^{17} m^2/s kinematic viscosity ($3 \cdot 10^{20}$ Pa s). The viscosities are higher than those estimated from laboratory experiments (AvéLallemant and Carter 1970; Goetze and Brace 1972; Ross and Nielsen 1978; Vetter 1978; Jacoby and Ranalli 1979). Note that we shall use the terms "lithosphere" and "asthenosphere" without quotes even if we refer to nothing but the high and low viscosity layers in our models.

Figure 1 shows, as might have been expected, that the highly viscous and thick lithosphere keeps the circulation from reaching the surface and concentrates it in the softer regions below. The lithosphere is caught motionless between

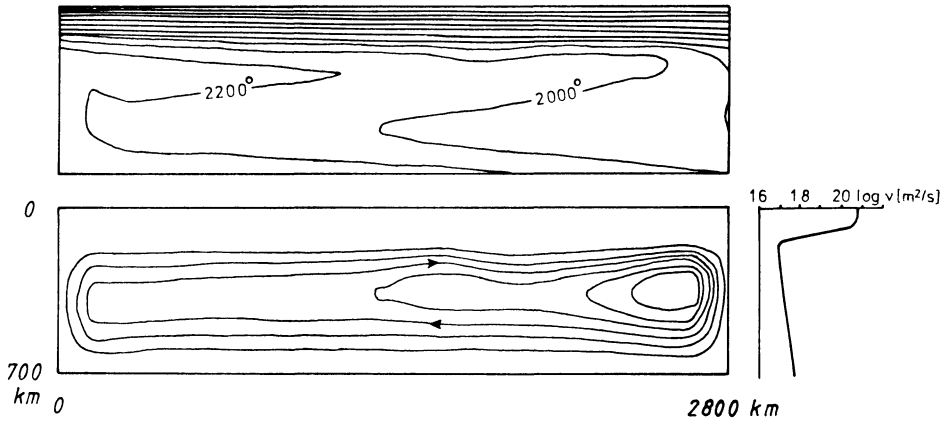

Fig. 1. Convection model with depth dependent viscosity $\eta(z)$ after McConnell (1968; model 62-12). $Ra \approx 3 \cdot 10^5$; heating from within $6.65 \cdot 10^{-8}$ W/m^3 and from below 12.56 mW/m^2. *Top*: isotherms in °C; *bottom*: stream lines; *right-hand side*: viscosity-depth function. Note that the high-viscosity lid does not participate in the circulation

the lateral boundaries, or better, between the neighbouring plates (because of the assumed mirror-image boundary condition). The lithosphere acts as a thermal insulator so that the mantle underneath heats up to unrealistically high temperatures of more than 2 000° C in the solution presented.

This model, with an effective Rayleigh number of 2.6×10^5 did not reach a steady state; instead the circulation oscillated irregularly with an approximate period of $8 \cdot 10^7$ years about a state which is presented in Fig. 1, with a relative amplitude of 20%. Oscillations are characteristic for convection at high *Ra* in the laboratory (Krishnamurti 1970a; b). There they are, however, a typical three-dimensional phenomenon which cannot be modelled with a two-dimensional scheme. Since the above period is that of particle revolution of the inner cell region, the oscillatory behaviour at least resembles that of real physical systems and does not appear to be an artefact of the numerical method.

The aspect ratio of the circulation (Fig. 1) is 4 or even $\gtrsim 5$ if the lid is subtracted. One must ask whether this high aspect ratio might be a numerical effect of the high-aspect-ratio mesh. Our contention is that this is not so. Heating largely from within stabilizes large-aspect ratio flow (Tozer 1967a; Tritton and Zarraga 1967; DeLaCruz 1970; Thirlby 1970) and so does viscosity layering below the lid (Richter and Daly 1978; Daly 1980). Our contention is supported by the following: A test with the same model, but heated entirely from below, failed to produce a stable single cell; after 500 million years of unsteady variation a steady three-cell pattern developed. Similar tests with constant, instead of layered, viscosity below the lid also failed in this way. Finally the circulation of Fig. 1 is itself probably on the brink of instability, as suggested by the bumps of the stream lines and isotherms. We do not however claim that our limited computational procedure allows us to define the point of cell instability precisely.

The above model is obviously not satisfactory. Neither were experiments with lithospheres of reduced viscosity and/or thickness. As found by Houston and DeBremaecker (1975), the less rigid plates participated in the convection currents, but not as rigid plates; rather they deformed internally.

A better way of simulating the lithosphere is to introduce a yield stress in the model or at least in critical regions, i.e. weakness zones (Kopitzke 1979). If the yield stress is passed during the computation, the viscosity at that location is reduced so that the material can yield and the shear stress is not exceeded in the next step. The yield stress is thus the upper limit of sustainable stress. It may not be a yield stress in the true physical sense but is meant to represent an average property of the weakness zone. In two lithospheric regions (stippled in Fig. 2) of the previous model the "yield stress" was set to 500 bar. The effect of this modification is seen clearly in Fig. 2. The lithosphere now partakes, without being deformed, in the convective circulation with a velocity of 2 cm/a. As demonstrated by the velocity depth profile (taken in the middle of the cell) the plate moves against resistance from the slower currents in the asthenosphere; it is not dragged by faster currents. The asthenosphere has become the zone of maximum shear.

The mean mantle temperature has dropped in the steady-state solution from the previous model to much lower values, about 830° C. This is low in the light of present estimates as e.g. Solomon (1976: $1\,100 \pm 100$° C in the low-velocity channel and $1\,300 \pm 150$° C near the olivine-spinel transition at 400 km depth) and Anderson (1980: 1 100–1 200° C, 100–400 km depth). It is also lower than most of Tozer's (1967a; b; personal communication, 1981) estimates based on convection theory and rheology. The lateral temperature variation computed is 200–300° C, characteristic of all our models with horizontal flow velocities of 1–2 cm/a and the assumed heat input. A more thorough discussion of these aspects follows after our results. The solution of Fig. 2 has a temperature inversion in the depth interval 200–400 km extending across nearly the whole length of the convection cell. This may preclude the small-scale Richter convection rolls (Richter and Parsons 1975), as argued by Kopitzke (1979), but it would not prevent instabilities of the boundary layers. Such a temperature inversion has not yet been resolved, except for an indication given by Anderson (1980) for the case that the seismic low-velocity zone consisted of dry lherzolite or eclogite.

Next, a viscosity-depth model was assumed with generally two orders of magnitude lower values than previously (Fig. 3). It was taken from a one-dimensional flow model with nonlinear rheology based on laboratory data (Jacoby and Ranalli 1979), but with one order of magnitude further reduction. The strain-related viscosity in this case cannot be directly transferred from one model to another; it just served us as a test case for a low-viscosity model. As above, we introduced weakness

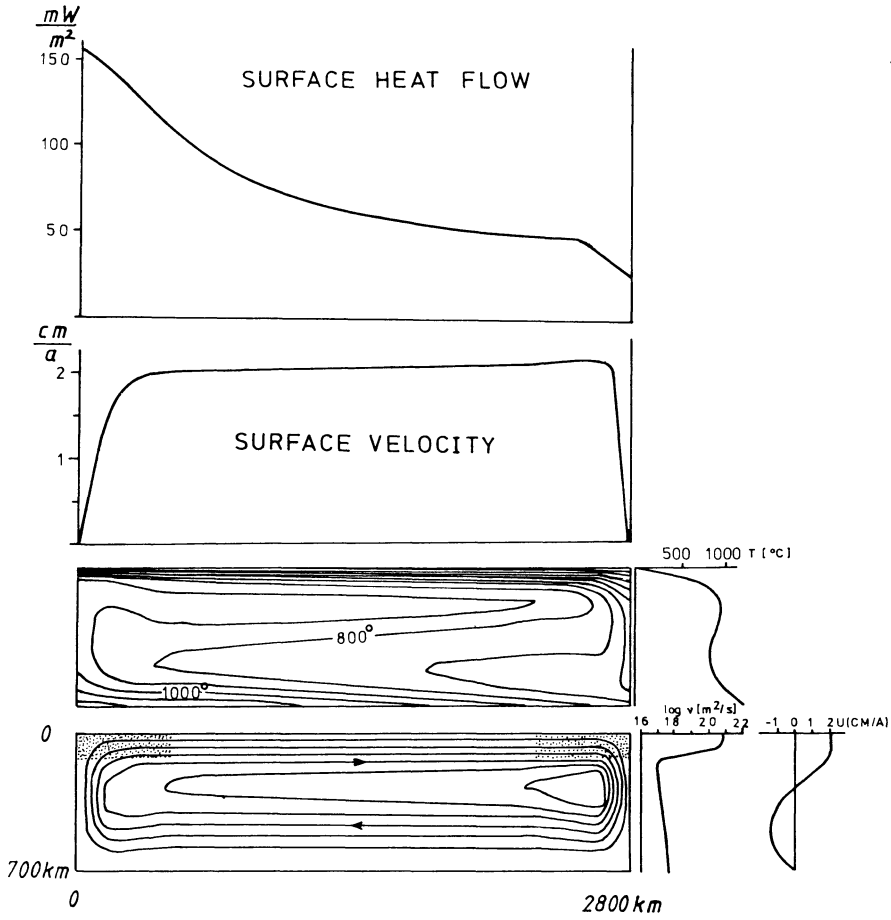

Fig. 2. Same as Fig. 1, but with yield stress (500 bar) assumed for stippled regions of lithosphere. $Ra \approx 1.5 \cdot 10^5$. *Center*: isotherms in °C with temperature-depth profile taken at center; *bottom*: stream lines with viscosity-depth profile and horizontal-velocity depth profile at center; *top*: surface velocity plotted versus x-axis and surface heat flow. Note that high-viscosity lid participates in circulation with nearly constant velocity

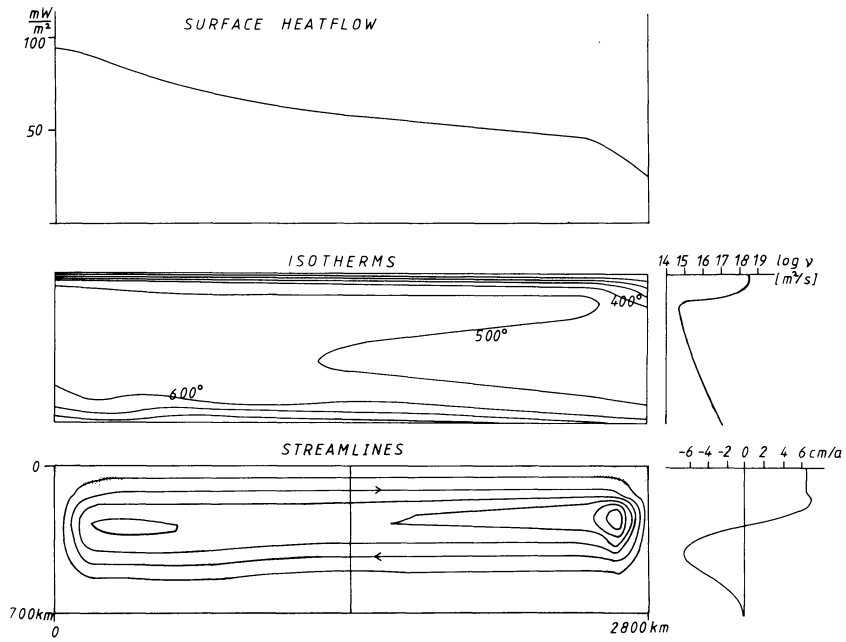

Fig. 3. Convection model with depth dependent vescosity $\eta(z)$ similar to one computed by Jacoby and Ranalli (1979) with weakened zones (*stippled*: $\nu = 10^{17}\,m^2/s$); heating as in Fig. 1; $Ra \approx 1.25 \cdot 10^7$. *Bottom*: stream lines, but not steady state; vertical profile of horizontal velocity at right-hand side; *center*: isotherms; viscosity-depth profile at right-hand side; *top*: surface heat flow

zones (stippled in Fig. 3) in which the viscosity was simply reduced to $10^{17}\,m^2/s$ (instead of by yield stress). In nature such a reduction of effective viscosity is achieved by fracturing, transient creep, plastic creep in narrow weakness zones, localised frictional heating, partial melting and thermal runaways (Schubert and Yuen 1978; Kaula 1980).

As the model of Fig. 1, this also did not reach the steady state. The circulation oscillated with a relative amplitude of 3% and a constant period of $4 \cdot 10^7$ years about the state shown. Again the period is about that of particle revolution in the inner cell region. Changing the length of the time steps by factors of 2 and 4 during execution did not

affect the period or amplitude of oscillation, supporting the view that the behaviour reflects physical, not numerical instability.

The low viscosities lead to relatively high velocities, about 6 cm/a horizontally in the lithosphere and asthenosphere and up to 25 cm/a in the descending current. This is nowhere excessive: a viscosity decrease of two orders of magnitude has resulted in a velocity increase of only a factor of 3. Remember that the two models differ only in viscosity and have the same heat input.

The lower viscosities have lead to much more efficient convection so that the driving temperature and density disturbance is strongly reduced. Correspondingly the average cell temperature has dropped to about 500° C and the lateral temperature difference to about 100° C. The temperature inversion has nearly vanished to only 10° C.

Comparison of the above models (Figs. 1, 2, 3) shows that the circulation pattern of the last one is somewhat intermediate between the former two: that of Figure 1 is characterized by asthenospheric currents driving, though ineffectively, the lithosphere; that of Fig. 2 is reversed, the lithosphere leading and thus driving the asthenospheric currents; in Fig. 3 the top asthenospheric currents are again faster, by a margin (0.5 cm/a), than the lithosphere (see velocity-depth profile taken at cell center). The lithosphere in this model is thus less "active" in the sense of being partly dragged by asthenospheric flow.

These models give us a clue to what determines the role of the lithosphere in the whole circulation. In the models the role is largely the result of the relative strength of coupling between the lithosphere and the asthenosphere, or the ratio of viscosity in the plate-decoupling zones and viscosity of the asthenosphere. Had we assumed a lower value than 10^{17} m^2/s for the stippled zones of Fig. 3, the lithosphere would again have moved faster than the asthenosphere. A systematic study of this aspect is deferred to a later time.

The above solutions for different kinds of coupling of the plates demonstrate the broad capability of our numerical method. The major conclusions are not affected by the crude treatment. We must, however, be cautious as to quantitative details, e.g. the exact transition points from one mode to another, the stability of cells, the precise relative velocities of plates and asthenosphere. A reason for caution is the poor, smeared-out representation of the boundary layers in a mesh of 35 km vertical spacing. These points will be discussed again below.

The following experiments were conducted with materials having viscosities that depend on temperature and pressure (Newtonian) or on temperature, pressure and shear stress (non-Newtonian). We wanted to investigate whether such rheologies would automatically give convection involving the lithosphere. Based on the review by Stocker and Ashby (1973) of linear and non-linear creep mechanisms, one may consider Nabarro-Herring creep, Coble creep, and diffusion-accommodated grain boundary sliding as linear processes and dislocation creep as a non-linear mechanism; they all contribute to the effective viscosity (Jacoby and Ranalli 1979):

$$\eta = 1 \Big/ \left(2 \; f \cdot \frac{D_{\text{eff}}\, \Omega}{k \cdot T \cdot d^2} + \frac{3^{\frac{n+1}{2}} A \cdot D_v \cdot b}{k\, T \mu^{n-1}} \; \tau^{n-1} \right). \tag{4}$$

The meaning of the quantities and the numerical values assumed are presented in Tables 1 and 2. The first term combines the linear creep mechanisms and the second term describes dislocation creep. Temperature and pressure dependence is mainly in the diffusivities:

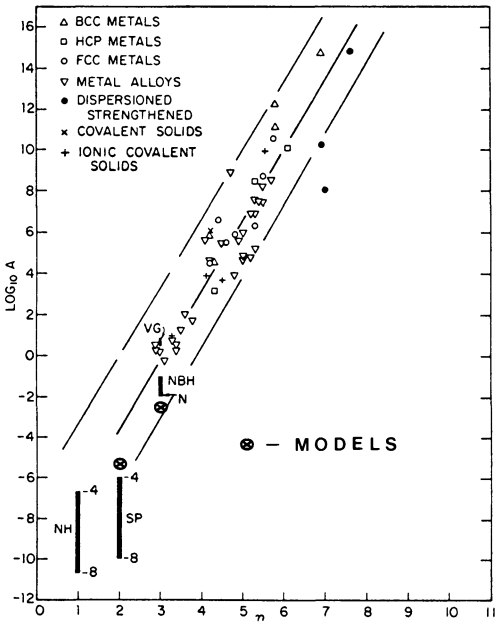

Fig. 4. Empirical relationship between Dorn's parameters A and n for various classes of metals (after Stocker and Ashby 1973) with the preferred values of our models added

$$D_v = D_{v0} \cdot \exp\left(-\frac{E_v + p\, V_v}{RT} \right);$$

$$D_{\text{eff}} = D_v (1 + \pi\, \delta / d \cdot D_B / D_v);$$

$$D_B = D_{v0} \exp\left(-\frac{E_B + p\, V_v}{RT} \right). \tag{5}$$

Similar rheologies have been investigated in boundary layer convection models of the upper mantle (Froidevaux and Schubert 1975; Schubert et al. 1976; Froidevaux et al. 1977; Schubert et al. 1978) and in convection models similar to ours (Rabinowicz et al. 1980; Daly 1980). Some of their results, e.g. concerning the effective viscosity, bear on our work and can be used as an additional test of our numerical method (see discussion, below).

The strong effect of temperature and stress in some of our models occasionally resulted in numerical, or indeed physical, instabilities. Since some of the rheological parameters responsible are in part not accurately known it seemed justified to vary them within plausible limits in order to achieve acceptable models: this mainly concerns grain size d, activation energy and volume E_v and V_v, and Dorn's parameters A and n. Our favoured values were $d = 10^{-3}$ m, $E_v = 5.4 \cdot 10^5$ J/mol, $V_v = 10^{-5}$ m^3/mol, and the value of n was varied between 1 and 3; A was adjusted to give plausible flow velocities. Our favoured values are plotted on the experimental data for n, A as summarised by Stocker and Ashby (1973) (Fig. 4) and fall within the experimental scatter.

First we tested models having *no* weakened lithospheric zones, hoping that stress concentrations combined with power-law creep ($n = 3$) might reduce the effective viscosity locally and decouple the surface plate. None of the many models investigated showed this effect, partly because the low temperatures dominated the rheology, but mainly because the expected instabilities cannot be represented in the coarse mesh. We

therefore again introduced weak zones. Now we located them 500 km from the lateral boundary so that subduction would be induced, but not at the boundary, i.e. not symmetrical (which it otherwise would be for reasons of computational symmetry). The crude method does not permit us to model detail, but the gross features can be studied. Furthermore, a series of tests demonstrated the need for some more decoupling of the descending flow by two narrow low-viscosity zones (stippled in Figs. 5–7) because otherwise the cold highly viscous material tended to stagnate. A viscosity of $5 \cdot 10^{16}$–$4 \cdot 10^{17}$ m^2/s in these weak zones did usually suffice for mobility to be regained. We are not happy about this manipulation, made in order to overcome the shortcomings of the crude mesh, but we also believe that nature, too, may provide some decoupling by narrow shear zones, local heating and melting, and at shallow depth, fracturing.

Figure 5 shows a model with linear T, p dependent rheology; the viscosity in the stippled regions is reduced to the constant value of 10^{17} m^2/s. The initial condition was constant temperature at the bottom, with a small perturbation to initiate the flow in the direction wanted. For 150 million years model time, the lithosphere participated actively in the currents, but the return flow progressively concentrated at greater depth. Although the plate velocity was rather slow (maximum 1 cm/a heating of the subducted material was even slower and viscosity became so high that the return flow of plate material became inhibited. Drift and subduction of the lithosphere choked (the velocity decreased to 1–2 mm/a). Convection shifted to sublithospheric depths and split up into four cells. The results looked satisfactory for only 45 million years running time, afterwards they differed from our picture of real Earth behaviour; but admittedly we know little about the long-term aspect of plate motion.

We do not want to overemphasise the particular time behaviour described. The ADI method used cannot resolve rapid temporary changes. If, however, the change during a time step is small, as is the case here, the computation should not be grossly wrong. The important point we wish to make is that the model with the rheology chosen does not convect in a single stable cell; the flow breaks up to a new steady state with several cells. A similar evolutionary behaviour was observed with essentially the same computational method by Torrance and Turcotte (1971) and Rabinowicz et al. (1980).

The above model with mainly temperature dependent rheology is apparently incapable of describing steady-state convection with subduction during long time spans. If such a behaviour, of which we cannot be entirely certain, is favoured, it is not simulated by the model, particularly for fast-moving plates. A possible escape from the dilemma is non-linear, i.e. shear stress dependent rheology by which the effective viscosity in cold subduction regions can be sufficiently reduced to permit a steady-state return flow.

Equations (4) and (5) with Dorn's parameters $n=2$, $A=3 \cdot 10^{-6}$ describe the creep laws assumed for the next model (Fig. 6); the viscosity in the stippled regions was set to $4 \cdot 10^{17}$ m^2/s. The result was the development of a steady-state convection cell with the lithosphere participating. It was about 80 km thick and thickening toward the region of descent. Below it a low-viscosity asthenosphere developed. Both drifted together at somewhat less than 2 cm/a. In the descending current, material from the lithosphere dropped at 0.5 cm/a while material from the asthenosphere flowed faster (0.9 cm/a). The figures quoted may be inaccurate by, say, 10%, but the general behaviour described seems significant.

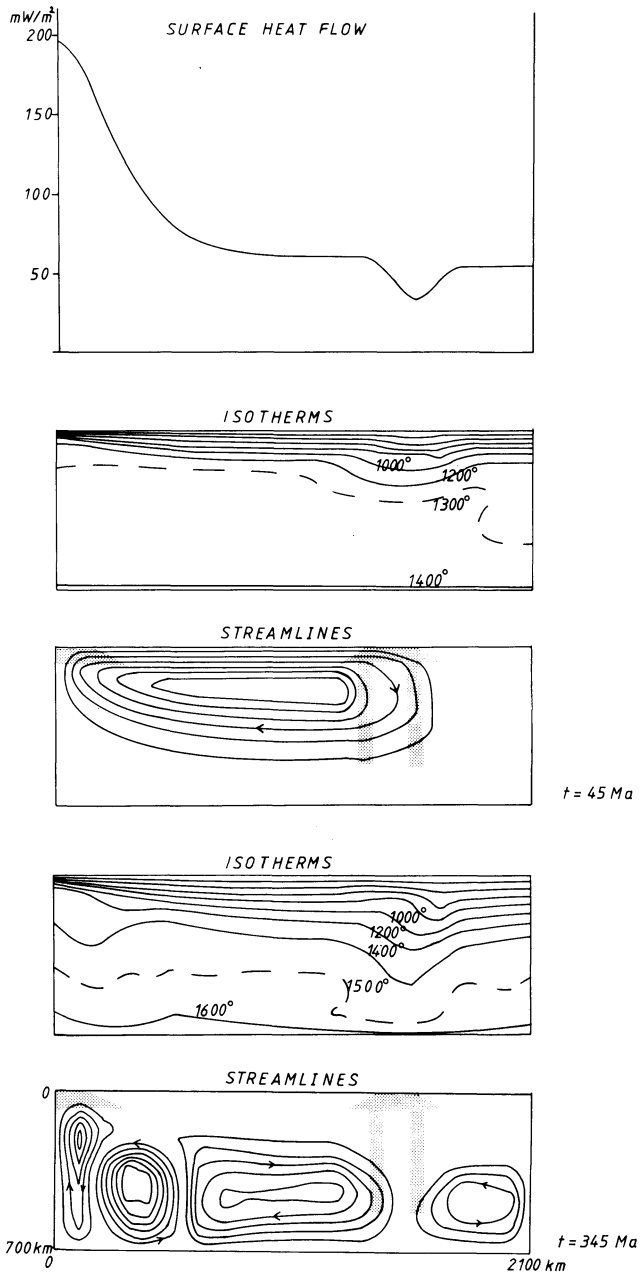

Fig. 5. Convection in a model with T, p dependent linear rheology with additional weakened zones (stippled) at two moments of time. At 45 million years the circulation encompasses the lithosphere (*upper part*: surface heat flow (*top*), isotherms (*center*), stream lines (*bottom*); after 345 million years the surface is stagnant and four cells have developed in the asthenosphere (*lower part*: isotherms (*top*) and stream lines bottom))

A comparison of the above two models demonstrates that the reduction of the effective viscosity by shear stress prevents freezing of the descending current which can then turn into a return flow. Power-law creep dominates in the lower part of the descending current as can be seen by comparing the weakly and the strongly deformed regions in the field of computed viscosities (Fig. 6).

Note that a secondary cell developed behind the subduction region. Such cells are expected to exist beneath the marginal basins, e.g. of the western Pacific, and may provide an explanation for the basins and their high heat flow and

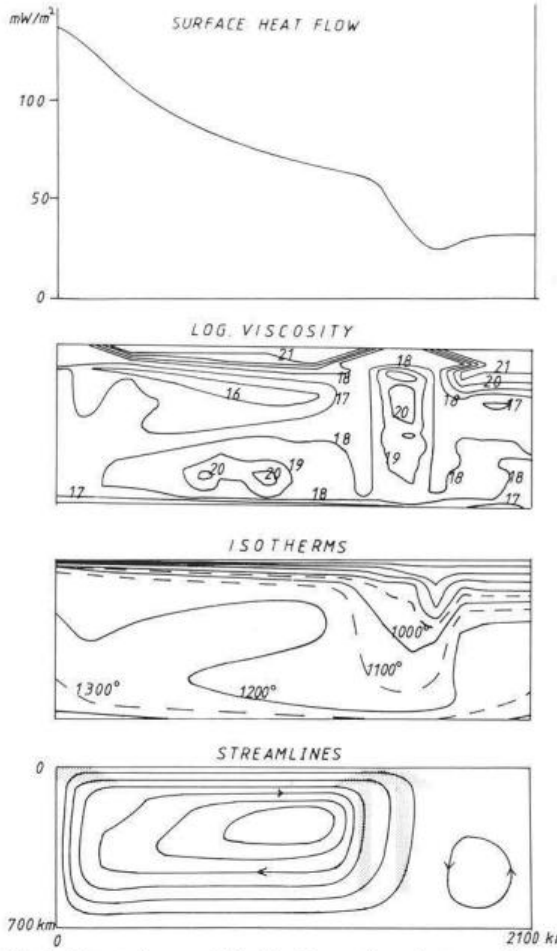

Fig. 6. Convection model with T, p, τ dependent non-linear rheology; Dorn's parameters $n=2$, $A=3\cdot10^{-6}$; weakened zones $\nu=4\cdot10^{17}\,m^2/s$; surface heat flow (*top*), isotherms (*second from bottom*), stream lines with surface velocity ~2 cm/a (*bottom*), computed viscosity (*second from top*) with weakened zones visible. Dissipation and adiabatic heating included; if not, lithosphere descent becomes stagnant after 100 million years (in a model not shown here)

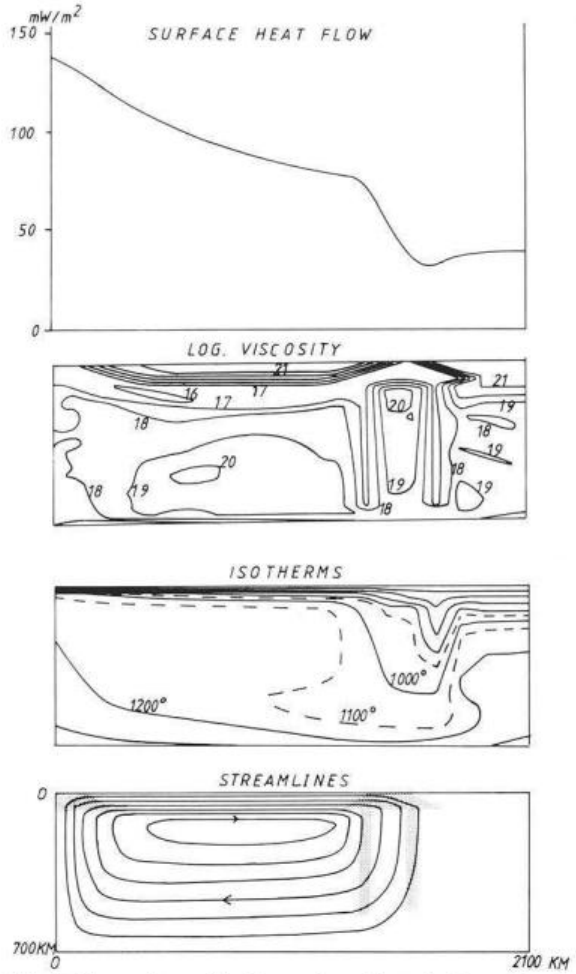

Fig. 7. Convection with T, p, τ dependent rheology: Dorn's parameters $n=3$, $A=4\cdot10^{-3}$; weakened zones $\nu=5\cdot10^{16}\,m^2/s$. The model was quasi-steady-state after 150 million years; surface velocity was ~3 cm/a. Arrangement of results as in Fig. 6. Note that the relatively higher temperatures were partly the result of a numerical heating excess (see text); the following model (Fig. 8) was computed to test whether similar results can be obtained with correct "physical" heating

volcanism (Andrews and Sleep 1974; Rabinowicz et al. 1980). In the previous model with linear viscosity (Fig. 5) such a cell did not develop until subduction had choked and the asthenospheric convection had broken up into several cells.

It must be remarked that the features of model Fig. 6 were the result not only of non-linear stress dependent rheology; the thermal effects of adiabatic compression and decompression as well as of dissipation helped to keep the lithosphere going. This was different from previous models where these terms were also included without success. For example, one model (not shown) differed from that of Fig. 6 only by not including these effects; during the first 100 million years a plate drifted actively but then slowed down progressively to 0.5 cm/a while asthenospheric velocities were 10 cm/a. Obviously, in the model of Fig. 6, the heating of the descending flow by adiabatic compression was an important mechanism reducing the effective viscosity. Dissipation acted in the same direction, being proportional to the product of shear stress and strain rate. It is interesting to note that such non-linear processes as dissipation and power-law creep appear to stabilize the flow in the models.

The final model we present (Fig. 7) differs from the previous one by the choice of Dorn's parameters: $n=3$, $A=4\cdot10^{-3}$, and by the viscosity in the (stippled) decoupling zones: $\nu=5\cdot10^{16}\,m^2/s$. In this model, in contrast to the previous one, the flow that developed in one direction was nearly restricted to the lithosphere while the return flow occurred at least partly in the asthenosphere. One of the reasons for this feature is probably that the strong non-linearity of the rheology promotes currents in which the zones of high shear rate and bending of the stream lines are spatially concentrated (into the asthenospheric shear zone). Another reason may be the more efficient decoupling in the stippled areas. Apart from the artificial aspects, the model generally simulates the lithosphere as an active part of the circulation rather well. Its velocity was 3 cm/a.

The temperatures appear to be quite in accord with what we know about the mantle, and this is coupled with realistic plate velocities. A close look reveals, however, an apparent heating excess of 35% resulting in an average surface heat flow of about 80 mW/m^2 (caused by inaccurate finite difference approximation of the partials in regions of highly vari-

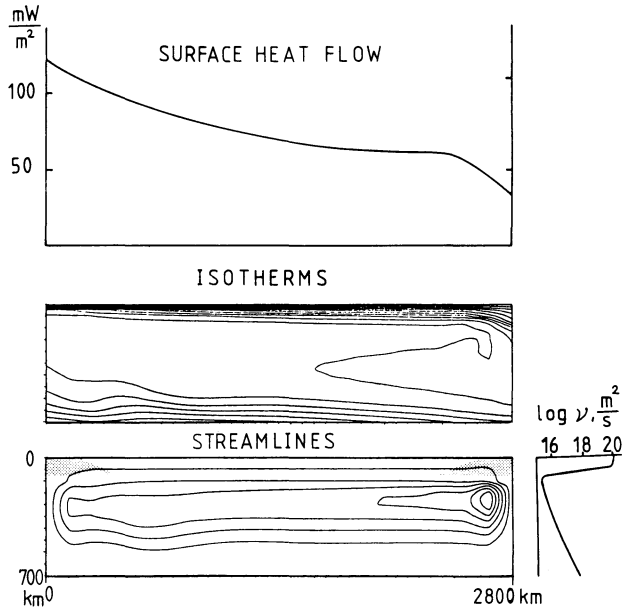

Fig. 8. Convection with depth-dependent viscosity $\eta(z)$, similar to that of Jacoby and Ranalli (1979); heat flow through bottom as in Fig. 1, internal heating raised to $9.4 \cdot 10^{-8}$ W/m^3 in order to add up to an average steady-state surface heat flow of 80 mW/m^2. *Bottom*: stream lines, viscosity-depth profile at righthand side; *center*: isotherms: *top*: surface heat flow

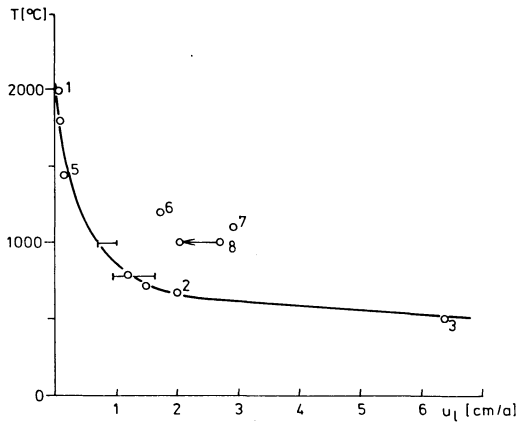

Fig. 9. Average model temperatures versus plate velocity u_l of models with aspect ratios 3 and 4. Not all models shown on diagram are discussed in paper (model numbers refer to Figures). *Arrow* points to position of model if scaling length L is increased (see text)

able rheology and strain rate). This happens to be closer to the oceanic average of 78 mW/m^2 (Sclater et al. 1980) than the 60 mW/m^2 assumed above. It was this heating excess that led to the higher temperatures.

Similar temperatures result if the total "physical" heating corresponds to a steady-state average heat loss of 80 mW/m^2 and dissipation is computed correctly. This is shown by the model of Fig. 8, which has simply a depth-dependent viscosity and weak zones ($4 \cdot 10^{16}$ m^2/s). The solution oscillated (relative amplitude $<3\%$, period $8 \cdot 10^7$ yr); the lithospheric velocity of 2.7 cm/a and the mean temperature of 1,012° are close to those of Fig. 7 (2.9 cm/a and 1 090°); there the low "physical" heat input and the high "numerical" dissipation seem thus to have cancelled to give, in a sense, a realistic model. By "realistic in a gross sense" we mean: large aspect ratio; nearly steady state; active participation of the lithosphere at plausible velocity, crudely subducting; acceptable mantle temperatures: all this obtained from a set of plausible assumptions (physics of the problem, material). Details, e.g. of viscosity distribution (Fig. 7), temperature and flow fields should be taken with a grain of salt; they are affected by the crude mesh, the numerics, and the artificially assumed weakness zones. We are therefore limited to drawing conclusions about the mantle only from the gross features of the results.

Discussion

In this section we wish to discuss more generally some aspects of temperature, rheology and viscosity, and flow patterns.

In most of our models (except Figs. 6–8) the total heat input was rather small by current knowledge. Correspondingly, the plate velocities and/or the average cell temperatures came out relatively low: <10 cm/a and less than 1 100°–1 300° C, respectively, which are believed to be realistic (Solomon 1976; Anderson 1980). Only as a result of insulation by a stagnant, strong lid (Fig. 1) did we observe high cell temperatures. As soon as plate motion makes convective heat transfer efficient, cell temperatures drop, in many models below the plausible range. In models with non-linear rheology, temperatures were closer to expectation, due to the heating excess which, as discussed above, had the right magnitude. If the temperatures are still considered too low, it should be remembered that the adiabatic gradient (or *Di*) is not well known and may be higher than assumed here: with the rheologies assumed, the viscosity would then drop, convection would become more efficient and temperatures would again drop in a self-regulating manner. The exact effect of varying the adiabatic gradient on self-regulation needs to be studied systematically.

Another reason for the relatively low temperatures and/or velocities may be our assumption of a shallow bottom to convection (700 km depth), as discussed by Schmeling (1980). The argument is as follows. All models (shown and not shown) computed with the same heat input and the same aspect ratio, but with different rheologies follow an empirical relationship of the form (Fig. 9):

$$u_1 \cdot (\bar{T} - T_{num}) = c \tag{6}$$

where u_1 is the lithosphere velocity, $\bar{T}$ is the average model temperature, T_{num} a constant related to the particular choice of the grid, and c is a constant depending only on the total heat input (and the aspect ratio), but not on rheology or viscosity. Low plate velocity and/or temperature means a low value of c; it does, however, increase with the dimensionless heat input $H = \mathscr{H} \cdot L^2/(\rho \cdot c_p \kappa_0 T_c)$. The models of Fig. 6 (20% increase) and Fig. 7 (35%) clearly lie above the curve of Fig. 9; increasing $\mathscr{H}$ in Fig. 8 by a factor of 4/3 (80 mW/m^2 over 60 mW/m^2) is equivalent to an equal increase of L^2 with heating unchanged. In that case the dimensional velocity drops to about 2 cm/a, as indicated by the arrow on Fig. 9. The model would still clearly lie above the curve for constant heat input. Thus empirically c (velocity × mean temperature) grows with L in the case of "mixed" heating from within and below, as has been found also by Kopitzke (1979).

The theoretical difficulties of treating the case of mixed heating do not arise in the case heated from below only. Here, however, mean velocity v and temperature fluctuation θ

do not depend on L to first approximation, if the superadiabatic temperature difference ΔT is fixed. The heat input is then (F. Busse, personal communication, 1981): $h = Nu\ k\ \Delta T$ (k = thermal conductivity); with $Nu \approx (Ra - Ra_c)^{\frac{1}{3}}/Ra_c^{\frac{1}{3}}$, $v \approx (Ra - Ra_c)^{\frac{1}{3}}\kappa/L \approx Ra_c^{\frac{1}{3}}\ h/(\Delta T \rho c_p)$, and $\theta \approx \Delta T(Ra - Ra_c)/Ra$, both independent from L. The fixed-ΔT case is, however, not relevant to our problem.

If higher mantle temperatures and plate velocities than in our shallow models are favored, e.g. by reliable inference of temperatures from observations, then, on the basis of the above discussion, deep-mantle convection must be favoured over shallow. This would also require that a considerable portion of the heating be internal, by radioactive decay and or by the heat lost in cooling of the Earth, i.e. by stored heat.

On the other hand, we may accept the relatively low temperatures we found. Tozer (1967a, b) pointed out that a self-regulating convection mechanism through T (and p, τ) dependent rheology without fixed temperature bounds may indeed adjust to temperatures as low as computed in our models. Some of the temperature estimates (Solomon 1976) may be biased toward high values as they sample volcanism. This cannot be said about Anderson's (1980) estimate based on average seismic Earth models and laboratory data on minerals; the suggested temperature range is correspondingly lower.

Because of the low numerical resolution, it would be valuable to compare our results (temperature, effective viscosity, flow patterns, Figs. 6, 7) with physically similar models, obtained with different techniques. The most relevant models seem to be those based on boundary layer theory, giving more accurate results in the boundary layer region, with similar rheological assumptions (Froidevaux and Schubert 1975; Schubert et al. 1976; Froidevaux et al. 1977; Schubert et al. 1978). The closest resemblance in physical assumptions seems to be between the model of our Fig. 7 and that of fig. 6 of Schubert et al. (1976); in both cases rheology is nonlinear with Dorn's parameter $n = 3$ and activation energy $E = 5.4 \cdot 10^5$ J/mol; see Table 1. We found a minimum viscosity increasing with age of the overlying lithosphere from $\lesssim 3 \cdot 10^{19}$ Pa s at ~ 90 km depth to $\lesssim 3 \cdot 10^{20}$ Pa s at ~ 150 km depth; their equivalent values are: $5 \cdot 10^{19}$ Pa s at 70 km depth (10 million years) and $\sim 10^{20}$ Pa s at 180 km (150 million years). The coarse mesh cannot, of course, resolve accurately the boundary layer structure, however, the comparison with the results of Schubert et al. (1976, Fig. 7) shows that the resolution does not lead to grossly wrong results. Crudely, we find the high-gradient zones of temperature and horizontal velocity to thicken with age from 50–80 km, and from 80–110 km, respectively; their equivalent values were 50–100 and 80–160 km, respectively. The smearing-out of the crude mesh seems mainly to give less variation, not so much to give a greater thickness. Part of the discrepancy in the horizontal velocities also comes from the different model assumptions for the bottom: in our model the return flow must be accommodated within 700 km depth: their assumption is that horizontal velocity approaches zero "at great depth". Apart from this the flow patterns are not dissimilar.

The above comparison does not prove our results correct, neither generally nor in specific details, but we find it encouraging that even the boundary layer, and that in the most non-linear case, was represented rather satisfactorily in our models. It thus appears that the gross features and the major conclusions we draw from them are quite reliable. This is not to be said about quantitative details generally, as discussed above, but we did not in any case ask for such details.

On the basis of our results, we cannot argue strongly for whole versus shallow mantle convection. The argument of Richter and McKenzie (1978) for shallow convection is mainly that the stress distribution in the descending slabs cannot easily be explained without a bottom at about 700 km depth (Isacks and Molnar 1971). Plausibly, however, a compressive resistance could also develop simply by a viscosity increase above and below 700 km without necessarily preventing the currents from extending deeper (Davies 1977; Jacoby 1978; Kopitzke 1979).

Conclusions

Our main conclusions are listed below.

1. Only by the introduction of weak zones into the lithosphere was it possible to simulate its drift as a rigid, i.e. undeformed, body. It thus seems that plate velocity is essentially controlled by the strength or weakness of the mechanical coupling with neighbouring plates as well as with the lower, more viscous parts of the upper mantle.

The coupling near the surface and in the mesosphere may, however, behave differently. If in the subduction zones some kind of shear instability (which cannot be modelled with our techniques) develops, the coupling will remain weak, maybe approximately steady-state (unless other processes, such as collision, interfere – see McKenzie 1969). In contrast, plate descent into the mesosphere increases the coupling progressively until it may inhibit the motion. Non-linear processes do, however, lessen this effect. Little can be said at present about such a phenomenon in nature, nor did our models that choked run for long enough, but the time lapse until a reactivation of plate motion would have been at least 10^9 a. Furthermore, our method is not applicable to the study of the time behaviour. It may be added, that our quasi-steady state models (e.g. Figs. 6, 7) remained so as long as the computation continued (500, 270 million years).

2. While the rheology of the plates themselves has turned out to be of major importance for the plate motions, that of the material below, apart from its generally low viscosity, is less important for the plate velocities. For viscosity variations of several orders of magnitude and for both linear and non-linear viscosity, the plate velocities varied by no more than 1–6 cm/a.

3. Mantle rheology is, however, important for the form of the return flow. Mostly we have obtained broad maxima of this flow at depths not shallower than 400 km, suggesting that in the earth it is not the asthenosphere which mainly carries the return flow. The asthenosphere is probably dragged with the plates to a considerable extent (see Fig. 6) or it is the zone of concentrated shear flow, an effect which is enhanced by non-linear rheology (see Figs. 5, 7). Besides the rheology assumed by us, other non-linear effects may further concentrate the shear; such effects include dissipation, partial melting and upward concentration of melt (which is assisted by the strong shear), and thermal runaways.

4. As discussed in the previous chapter, we obtained low temperatures and/or plate velocities, even when the heat input was realistic. The average temperature and velocity are coupled through the heat input and cell geometry (fixed in our models or only slightly varied); the non-dimensional heat input can be increased by increasing the depth or the general

size of the cell; dimensions of $6\,000 \times 2\,000\,km^2$ or even $9\,000 \times 3\,000\,km^2$ (instead of $2\,100 \times 700\,km^2$) may thus be preferred. For this it would not be critical if the viscosity in the lower mantle increases by one to even three orders of magnitude.

The low temperatures may, however, be realistic estimates of the average upper-mantle temperatures. Our experiments suggest that the mantle will convect strongly at such temperatures, if the thermal and mechanical upper boundary layers are decoupled piecewise at their margins, and are thus free to move. If the surface becomes stagnant, the interior convects at much higher temperature because the heat loss is inhibited. In the earth's upper mantle temperature may rise locally, but not to as high values as in the lidded case; hot spots or volcanic spots may be witnesses of local temperature anomalies and should therefore be taken with caution in estimating upper-mantle temperatures.

5. The importance of decoupling for the whole dynamical problem, plate motions, temperature and thermal evolution, makes it urgent to study the decoupling mechanisms thoroughly. It appears possible that besides the mechanisms mentioned earlier (yield stress, fracturing, transient creep, plastic creep on faults, frictional heating, local melting, thermal runaways), and for some of these mechanisms, the presence or absence of minor volatile constituents, particularly water, may be of paramount importance. The fact that the earth's atmosphere and lithosphere are moist, in contrast to Venus that is dry, may explain the great difference of the surfaces of these two, otherwise rather similar planets (H. Spetzler, personal communication, 1981).

6. A considerable temperature inversion usually developed in the convection cells, amounting to 100–200 K if the effective viscosity was of the order of $10^{17}\,m^2/s$, but only to some 10 K for $10^{15}\,m^2/s$. The inversion increases as the plate motions are facilitated by reduced coupling. This feature, if relevant to the earth, may stabilise the large-scale mantle flow (Kopitzke 1979) and inhibit smaller-scale convection rolls as proposed by Richter (1973a), but it would enhance boundary layer instabilities, such as rising plumes. The large-scale flow may also become destabilised if plates grow to an excessive size, which seems possible if plate size is largely determined by its growth and destruction rates at existing ridges and trenches, leading to a multiplicity of horizontal scales (Richter and Daly 1978). Destabilisation would be the consequence of the inefficient heat loss, since only the generation and destruction of the plates transfer heat convectively and elsewhere heat loss is by conduction through the boundary layer. There is evidence from bathymetry, gravity, and the geoid for three-dimensional flow below the plates (McKenzie et al. 1980). Three-dimensional instabilities below the Pacific may be enhanced by the circumstance that the Pacific is shrinking; hence the upper mantle may be more stagnant (Hager and O'Connell 1978; Grohmann 1980) than a simple two-dimensional model of return flow would suggest.

Acknowledgements. Helpful critical comments on earlier drafts of this paper were provided by F. Busse, D.A. Tozer, and an anonymous reviewer. U. Christensen (formerly: Kopitzke) gave us an earlier version of the computer program. We have profited from discussions with U. Christensen, J.C. DeBremaecker, S.F. Daly, H. Spetzler, D.P. McKenzie, G. Schubert, T. Spohn, and others. We like to thank W. Mahler for drafting the figures and I. Hörnchen for typing the manuscript. The computations were done at Hochschulrechenzentrum, University of Frankfurt. Deutsche Forschungsgemeinschaft gave us financial support (grant Ja 258/6).

References

Anderson, O.L.: The temperature profile of the upper mantle. J. Geophys. Res. **85**, 7003–7010, 1980

Andrews, D.J.: Numerical simulation of sea-floor spreading. J. Geophys. Res. **77**, 6470–6481, 1972

Andrews, D.J., Sleep, N.H.: Numerical modeling of tectonic flow behind island arcs. Geophys. J. R. Astron. Soc. **38**, 237–251, 1974

Artyushkov, E.V.: Gravitational convection in the interior of the earth. Izv. Earth Phys. **9**, 3–17, 1968 (trans. J. Büchner)

AvéLallemant, H.G., Carter, N.L.: Syntectonic recrystallisation of olivine and modes of flow in the upper mantle. Geol. Soc. Am. Bull. **81**, 2203–2220, 1970

Bénard, H.: Les tourbillons cellulaires dans une nappe liquide. Rev. Gen. Sci. **11**, 1261–1271, 1900

Busse, F.H.: On the stability of two-dimensional convection in a layer heated from below. J. Math. Phys. **46**, 140–150, 1967

Busse, F.H., Whitehead, J.A.: Instabilities of convection rolls in high Prandtl number fluid. J. Fluid Mech. **47**, 305–320, 1971

Chandrasekhar, S.: The thermal instability in spherical shells. Phil. Mag., ser. 7, **44**, 233–241, 1953

Chandrasekhar, S.: Hydrodynamic and Hydromagnetic Stability. Oxford, Clarendon Pr.: 1961

Chapman, D.S., Pollack, H.N.: Global heat flow: A new look. Earth Planet. Sci. Lett. **28**, 23–32, 1975

Chapple, W.M., Tullis, T.E.: Evaluation of the forces that drive the plates. J. Geophys. Res. **82**, 1967–1984, 1977

Daly, S.F.: The vagaries of variable viscosity convection. Geophys. Res. Lett. **7**, 841–844, 1980

Davies, G.F.: Whole mantle convection and plate tectonics. Geophys. J. R. Astron. Soc. **49**, 459–486, 1977

DeBremaecker, J.C.: Convection in the earth's mantle. Tectonophysics **41**, 195–208, 1977

DeLaCruz, S.: Asymmetric convection in the upper mantle. Rev. Union. Geofis. Mexico. **10**, 49–56, 1970

Forsyth, D., Uyeda, S.: On the relative importance of the driving forces of plate motion. Geophys. J. R. Astron. Soc. **43**, 163–200, 1975

Foster, T.D.: Convection in a variable viscosity fluid heated from within. J. Geophys. Res. **74**, 685–693, 1969

Froidevaux, C., Schubert, G.: Plate motion and structure of the continental asthenosphere: a realistic model of the upper mantle. J. Geophys. Res. **80**, 2553–2564, 1975

Froidevaux, C., Schubert, G., Yuen, D.A.: Thermal and mechanical structure of the upper mantle: a comparison between continental and oceanic models. Tectonophysics **37**, 233–246, 1977

Gebrande, H.: Ein Beitrag zur Theorie thermischer Konvektion im Erdmantel mit besonderer Berücksichtigung der Möglichkeit eines Nachweises mit Methoden der Seismologie. Diss. München, 1975

Goetze, C., Brace, W.F.: Laboratory observations of high-temperature rheology of rocks. Tectonophysics **13**, 583–600, 1972

Grohmann, N.: Die 2-Scale Zellularkonvektion. Untersuchung über die Zusammenhänge zwischen Orogenese, Kontinentaldrift und Magmatismus. Diss. München, 1980

Hager, B.H., O'Connell, R.J.: Subduction zone dip angles and flow driven by plate motion. Tectonophysics **50**, 111–133, 1978

Harper, J.F.: On the driving forces of plate tectonics. Geophys. J. R. Astron. Soc. **40**, 465–474, 1975

Houston, M.H., DeBremaecker, J.C.: ADI solution of free convection in variable viscosity fluid. J. Comp. Phys. **16**, 221–239, 1974

Houston, M.H., DeBremaecker, J.C.: Numerical models of convection in the upper mantle. J. Geophys. Res. **80**, 742–751, 1975

Isacks, B., Molnar, P.: Distribution of stresses in the descending lithosphere from a global survey of focal mechanism solutions of mantle earthquakes. Rev. Geophys. Space Phys. **9**, 103–174, 1971

Jacoby, W.R.: Instability in the upper mantle and global plate movements. J. Geophys. Res. **75**, 5671–5680, 1970

Jacoby, W.R.: One-dimensional modelling of mantle flow. Pure Appl. Geophys. **116**, 1231–1249, 1978

Jacoby, W.R., Ranalli, G.: Non-linear rheology and return flow in the mantle. J. Geophys. **45**, 299–317, 1979

Jeffreys, H.: The stability of a layer of fluid heated below. Philos. Mag. **57** (2), 833–844, 1926

Kaula, W.M.: Material properties for mantle convection consistent with observed surface fields. J. Geophys. Res. **85**, 7031–7044, 1980

Kopitzke, U.: Finite element convection models: Comparison of shallow and deep mantle convection, and temperatures in the mantle. J. Geophys. **46**, 97–121, 1979

Krishnamurti, R.: On the transition to turbulent convection. 1. The transition from two to three dimensional flow. J. Fluid Mech. **42**, 295–307, 1970a

Krishnamurti, R.: On the transition to turbulent convection. 2. The transition to time dependent flow. J. Fluid Mech. **42**, 309–320, 1970b

McConnell, R.K.: Viscosity of the mantle from relaxation time spectra of isostatic adjustment. J. Geophys. Res. **73**, 7089–7105, 1968

McKenzie, D.P.: Speculations on the consequences and causes of plate motions. Geophys. J. R. Astron. Soc. **18**, 1–32, 1969

McKenzie, D.P.: Surface deformation, gravity anomalies and convection. Geophys. J. R. Astron. Soc. **48**, 211–238, 1977

McKenzie, D.P., Watts, A., Parsons, B., Roufosse, M.: Planform of mantle convection beneath the Pacific Ocean. Nature **288**, 442–446, 1980

Minster, J.B., Jordan, T.H., Molnar, P., Haines, E.: Numerical modeling of instantaneous plate tectonics. Geophys. J. R. Astron. Soc. **36**, 541–576, 1974

Minster, J.B., Jordan, T.H.: Present-day plate motions. J. Geophys. Res. **83**, 5331–5354, 1978

Morgan, W.J.: Convection plumes in the lower mantle. Nature **230**, 42–43, 1971

Parmentier, E.M., Turcotte, D.L., Torrance, K.E.: Studies of finite amplitude non-Newtonian thermal convection with application to convection in the earth's mantle. J. Geophys. Res. **81**, 1839–1846, 1976

Rabinowicz, M., Lago, B., Froidevaux, C.: Thermal transfer between the continental asthenosphere and the oceanic subducting lithosphere: its effect on subcontinental convection. J. Geophys. Res. **85**, 1839–1853, 1980

Rayleigh, J.W.S.: On convection currents in a horizontal layer of fluid when the higher temperature is on the under side. Philos. Mag. **VI**, ser. 32, 529–546, 1916

Richardson, R.M., Solomon, S.C., Sleep, N.H.: Tectonic stress in the plates. Rev. Geophys. Space Phys. **17**, 981–1019, 1979

Richter, F.M.: Dynamical models for sea floor spreading. Rev. Geophys. Space Phys. **11**, 223–287, 1973a

Richter, F.M.: Finite amplitude convection through a phase boundary. Geophys. J. R. Astron. Soc. **35**, 265–276, 1973b

Richter, F.M., Daly, S.F.: Convection models having a multiplicity of large horizontal scales. J. Geophys. Res. **83**, 4951–4956, 1978

Richter, F.M., McKenzie, D.P.: Simple plate models of mantle convection. J. Geophys. **44**, 441–471, 1978

Richter, F.M., Parsons, B.: On the interaction of two scales of convection in the mantle. J. Geophys. Res. **80**, 2529–2541, 1975

Roberts, P.H.: Convection in horizontal layers with internal heat generation. Theory. J. Fluid Mech. **30**, 33–49, 1967

Ross, J.V., Nielsen, K.C.: High temperature flow of wet polycrystalline enstatite. Tectonophysics **44**, 233–261, 1978

Schmeling, H.: Numerische Konvektionsrechnungen unter Annahme verschiedener Viskositätsverteilungen und Rheologien im Mantel. Diplomarb. Frankfurt, 1979 - also: Ber. Inst. Met. Geophys. Un. Frankfurt, Nr. **41**, 1980

Schubert, G., Turcotte, D.L.: Phase changes and mantle convection. J. Geophys. Res. **76**, 1424–1432, 1971

Schubert, G., Yuen, D.A., Turcotte, D.L.: Role of phase transitions in a dynamic mantle. Geophys. J. R. Astron. Soc. **42**, 705–735, 1975

Schubert, G., Yuen, D.A.: Shear heating instability in the earth's upper mantle. Tectonophysics **50**, 197–205, 1978

Schubert, G., Froidevaux, C., Yuen, D.A.: Oceanic lithosphere and asthenosphere: thermal and mechanical structure. J. Geophys. Res. **81**, 3525–3540, 1976

Schubert, G., Yuen, D.A., Froidevaux, C., Fleitout, L., Souriau, M.: Mantle circulation with partial shallow return flow: effects on stresses in oceanic plates and topography of the sea floor. J. Geophys. Res. **83**, 745–758, 1978

Sclater, J.G., Jaupart, C., Galson, D.: The heat flow through the oceanic and continental crust and the heat loss of the earth. Rev. Geophys. Space Phys. **18**, 269–311, 1980

Solomon, S.C.: Geophysical constraints on radial and lateral temperature variations in the upper mantle. Am. Mineral. **61**, 788–803, 1976

Solomon, S.C., Sleep, N.H., Richardson, R.M.: On the forces driving plate tectonics: Inferences from absolute plate velocities and intra-plate stress. Geophys. J. R. Astron. Soc. **42**, 769–801, 1975

Stocker, R.L., Ashby, M.F.: On the rheology of the upper mantle. Rev. Geophys. Space Phys. **11**, 391–426, 1973

Takeuchi, H., Sakata, S.: Convection in a mantle with variable viscosity. J. Geophys. Res. **75**, 921–927, 1970

Thirlby, R.: Convection in an internally heated layer. J. Fluid Mech. **44**, 673–693, 1970

Torrance, K.E., Turcotte, D.L.: Structure of convection cells in the mantle. J. Geophys. Res. **76**, 1154–1161, 1971

Tozer, D.C.: Some aspects of thermal convection theory for the earth's mantle. Geophys. J. R. Astron. Soc. **14**, 395–402, 1967a

Tozer, D.C.: Towards a theory of thermal convection in the mantle. In: The Earth's Mantle, T.F. Gaskell, ed.: pp. 327–353. New York: Academic Press 1967b

Tritton, D.J., Zarraga, M.N.: Convection in horizontal layers with internal heat generation, Experiments. J. Fluid Mech. **30**, 21–31, 1967

Turcotte, D.L., Torrance, K.E., Hsui, A.T.: Convection in the earth's mantle. Meth. Comp. Phys. **13**, 431–454, 1973

Vetter, U.R.: Stress and viscosity in the asthenosphere. J. Geophys. **44**, 231–244, 1978

Zienkewicz, O.L.: The Finite Element Method in Engineering Science. London: McGraw-Hill 1971

Received February 2, 1981, Revised version July 15, 1981
Accepted September 16, 1981